PERGAMON

International Journal of Solids and Structures 38 (2001) 1355–1367

INTERNATIONAL JOURNAL OF SOLIDS and STRUCTURES

www.elsevier.com/locate/ijsolstr

Plastic hinges development and crack stability analysis in a circular ring

Lih-Jier Young *

Department of Applied Mathematics, Chung-Hua University, 30 Tung-shiang, Hsin-Chu 30067, Taiwan, ROC

Received 13 June 1999

Abstract

The primary purpose of this work is to demonstrate that the location of a crack can strongly affect the sequence of plastic hinge development which in turn affects crack stability of a structure. A specific example of an elastic–plastic ring loaded with diametrically opposite concentrated loads is employed to investigate these effects. The method used is based on elastic superposition to obtain the elastic–plastic behavior and to evaluate the crack stability with plastic hinges present.

Keywords: Plastic hinge; Crack stability; *J*-integral

1. Introduction

In the analysis of limit loads, that is, the final collapse loads of plane structures, a rigid-plastic analysis is most often employed. The limit load is looked upon as the ''failure'' load of the structure. However, if a crack is present, instability of the crack may intercede at loads less than the limit load to induce ''premature failure''. The analysis of crack instability prior to (or at) first yield load has been the subject of a great deal of fracture mechanics literature.

On the other hand, elastic–plastic analysis of statically indeterminate structures of long slender members in bending, from first yield load to limit load, involves a sequential formation of plastic hinges at intermediate loads. The total member of plastic hinges becomes the degree of statical indeterminacy plus one at collapse. It is the objective of this paper to demonstrate that the location of the crack can strongly affect the sequence of plastic hinge development, as well as the crack location, affects crack stability. In order to clearly demonstrate these effects, the specific example of an elastic–plastic ring loaded with diametrically opposite concentrated loads is adopted.

Such a ring is three times redundant so that the final collapse mechanism requires four plastic hinges. The final collapse mechanism is itself always regarded as unstable (neglecting hardening) and can be analyzed by simple rigid-plastic analysis, so it is of little interest here. However, the analysis of the sequence of formation of the first three plastic hinges, and the effects of crack location on that sequence and crack

* Fax: +886-3-537-3771.

0020-7683/01/$ - see front matter
PII: S0020-7683(00)00095-0

stability will require elastic–plastic analysis. The double symmetry of the example selected will simplify the analysis and allows reasonable analytical solution through elastic superposition of fundamental cases to obtain the elastic–plastic behavior (with hinges), as well as crack stability assessment as hinges sequentially form. It is believed that this analytical method will clarify all assumptions for the reader, which might be left unclear if a fully numerical method such as finite element analysis was employed. Indeed, the superposition method will especially greatly enhance the understanding of the indeterminate structure effects on crack stability.

With these objectives in mind, the analysis shall proceed to establishing the conditions for development of the first, second, and third plastic hinges, respectively, and later to the conditions for crack instability.

2. Development of a first plastic hinge

The example chosen of a cracked ring with diametrically opposite concentrated loads is shown schematically in Fig. 1.The ring and its loading are doubly symmetric, indicated by ℄, except for the crack loaded by α. The mean radius of the ring is R and its radial thickness is t, and it will be assumed to be of uniform unit thickness perpendicular to its plane. P is the load and θ locates any section around the ring. It shall be assumed that the ring is long and slender, $R/t \geqslant 10$, so that deformation due to in-plane bending is the only significant deformation. Moreover, it shall be assumed that the moment, M, versus curvature changes, $1/\rho - 1/R$, relationship of elements of the ring are ideally elastic–plastic as in Fig. 2, following the solid curve, where plastic hinge formation occurs upon reaching the fully plastic moment, M_p. For the cracked element, the same assumption is made except that the reduced hinge moment will be denoted by M_{pCR}. The crack depth, a, if not otherwise specified, will be taken to be $a = 0.3t$, so that assuming plane stress constraint at the cracked section plastic hinge, then $M_{pCR}/M_p \approx 0.5$ for illustrative purposes. Now, in order to attempt to find the load, P_1, at which the first hinge forms and its location, it is noted that the ring

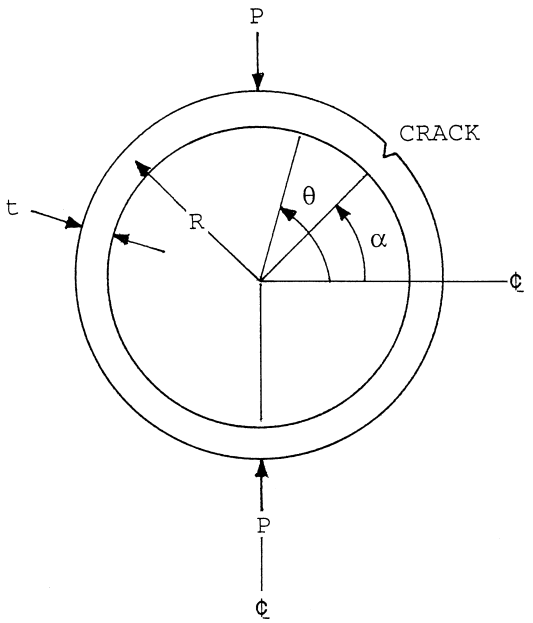

Fig. 1. Cracked ring with diametrically opposite concentrated loads.

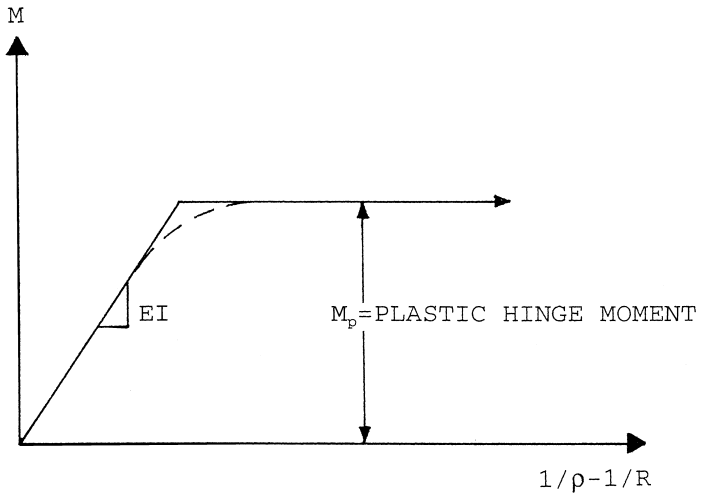

Fig. 2. Relationship of moment and curvature changes.

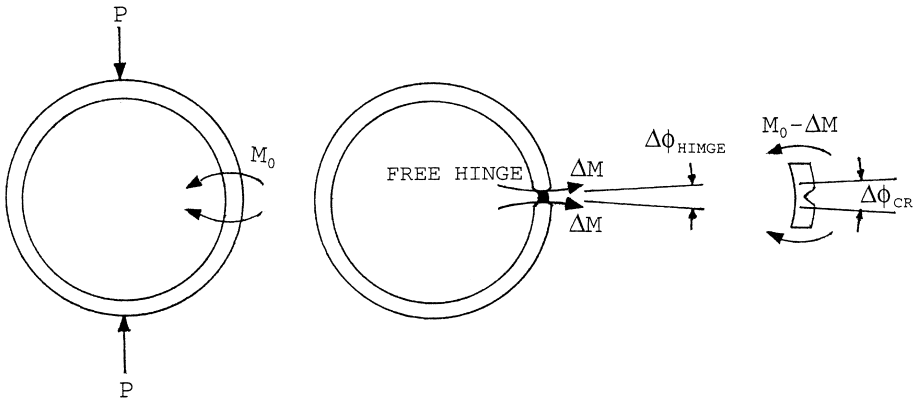

Fig. 3. Crack at $\alpha = 0°$.

can be analyzed as completely elastic up to that load. As a first approximation of the moments in a cracked elastic ring, the internal moments, M_0, in an "uncracked" ring as in Fig. 3 might be used. The elastic solution for the uncracked ring gives the results for M_0/PR in Table 1. However, the crack reduced the stiffness of the ring at the cracked section, causing a redistribution of the moment in the ring. This redistribution can be analyzed by the superposition method in Fig. 3.

In Fig. 3, the crack is taken to be at $\alpha = 0°$, a point of reasonably large moment, M_0, as noted from Table 1. Having a crack at this location imposes a large moment on the cracked element that should be relaxed by some unknown amount, ΔM, because of the extra rotation at the crack site, $\Delta\phi_{CR}$, imposing that same

Table 1
The uncracked ring (values repeat in each quadrant)

θ	0°	15°	30°	45°	60°	75°	90°
M_0/PR	0.182	0.165	0.115	0.036	−0.068	−0.189	−0.318

rotation on a ring hinged at the crack site results in the reduced moments, ΔM. To determine the proper reductions, ΔM analysis of the hinged ring cracked element must be done equating the angle changes; that is

$$\Delta\phi_{\mathrm{HINGE}} = \Delta\phi_{\mathrm{CRACK}}. \tag{1}$$

Table 2 shows the values of the corrected moment, M, around the ring including the elastic stiffness reduction at the cracked section for a/t ratios of 0.3, 0.4, and 0.5, also including differences in M_{pCR} due to these larger crack size ratios.

Inspecting Table 2 and comparing it with Table 1, it is noted that for $a/t = 0.3$, the relaxation of moments caused by the crack's elastic stiffness reduction is 4% or less, but for deeper cracks such as $a/t = 0.5$, the relaxation is as much as 30%. Nevertheless, if we wish to predict the location of the first plastic hinge, it can be done by comparing the ratios of the elastic moment at the crack ($\theta = 0°$), M_{CR} to the maximum moment in the uncracked part of the ring, $M_{\max}$ (all at $\theta = 90°$) with the limit moment ratios, $M_{\mathrm{pCR}}/M_{\mathrm{p}}$. The conclusion is that the crack location ($\alpha = 0°$) is the first hinge location for a/t of 0.3 and greater, otherwise it will be the loading point ($\theta = 90°$). These comparisons are shown in Table 3.

It is of interest to note from Table 3 that if a crack smaller than $a/t = 0.25$ were present in a ring prior to loading and if the crack grows during application of the loading to development of the first hinge, then the anticipated first hinge site might switch due to that growth. However, it then would be expected that second hinges would form at the originally expected locations with little additional loading. But beyond this comment, the effects of crack growth will be left for later work.

The relative load at which first hinges form is also of interest here. From Table 1, for an uncracked ring, the maximum moment is at the load point ($\theta = 90°$), and when that moment reaches M_{p}, the first hinge forms or

$$P_{\mathrm{I}} = \frac{M_{\mathrm{p}}}{(0.318)R} = \frac{\pi M_{\mathrm{p}}}{R}, \tag{2}$$

where P_{I} is thus the first hinge load of an uncracked ring or the largest, first hinge load, P_1, possible for a cracked ring. From Table 3, it is noted that for small cracks $a/t < 0.3$ (and $\alpha = 0°$), the first hinge is at the load point or $P_1 = P_{\mathrm{I}}$. However, for $a/t \geqslant 0.3$, the first hinge is at the crack location where the hinge moment is reduced by $M_{\mathrm{pCR}}/M_{\mathrm{p}}$. For that circumstance,

Table 2
θ and values of M/PR (for $\alpha = 0°$, and $R/t = 10$)

a/t	θ								$M_{\mathrm{pCR}}/M_{\mathrm{p}}$	P_1/P_{I}
	0°	15°	30°	45°	60°	75°	90°	180°		
0.3	0.177	0.160	0.111	0.032	−0.070	−0.189	−0.316	0.190	0.49	0.88
0.4	0.164	0.147	0.099	0.022	−0.078	−0.194	−0.319	0.197	0.36	0.70
0.5	0.136	0.120	0.074	0.000	−0.096	−0.208	−0.328	0.209	0.25	0.58

Table 3
Values of $M_{\mathrm{CR}}/M_{\max}$ and $M_{\mathrm{pCR}}/M_{\mathrm{P}}$ for $\alpha = 0°$

a/t	$M_{\mathrm{CR}}/M_{\max}$	$M_{\mathrm{pCR}}/M_{\mathrm{p}}$	$\alpha = 0°$
0.1	0.57→	0.81	First hinge at load point
0.2	0.57→	0.64	
0.3	0.56←	0.49	First hinge at crack
0.4	0.51←	0.36	
0.5	0.41←	0.25	

Table 4
θ and values of M/PR (for $a/t = 0.3$, and $R/t = 10$)

α	θ								P_1/P_I		First hinge
	0°	15°	30°	45°	60°	75°	90°	180°			
0°	*0.177*	0.160	0.111	0.032	−0.070	−0.189	−0.316	0.190	0.88	0°	At crack
15°	0.177	*0.160*	0.110	0.031	−0.072	−0.190	−0.317	−0.189	0.97	15°	At crack
30°	0.178	0.160	*0.109*	0.031	−0.072	−0.192	−0.318	0.188	1.00	90°	At M_{max}
45°	0.178	0.160	0.109	*0.031*	−0.072	−0.191	−0.318	0.186	1.00	90°	At M_{max}
60°	0.178	0.160	0.109	0.031	*−0.072*	−0.191	−0.318	0.186	1.00	90°	At crack
75°	0.182	0.163	0.110	0.032	−0.073	*−0.194*	−0.323	0.186	0.80	75°	At crack
90°	0.184	0.164	0.113	0.032	−0.073	−0.193	*−0.321*	0.184	0.78	90°	Both
	Outside crack					Inside crack					

Italicized terms indicate diagonal crack location.

$$P_1 = \frac{M_p}{\left(\frac{M}{PR}\right)R}\frac{M_{pCR}}{M_p}, \tag{3}$$

where (M/PR) are the appropriate values in tables such as in Table 3. Consequently, the ratio by which the first hinge load is reduced in a cracked ring where the hinge occurs at the crack is

$$\frac{P_1}{P_I} = \frac{(0.318)}{\left(\frac{M}{PR}\right)}\frac{M_{pCR}}{M_p}. \tag{4}$$

The last column in Table 2 is obtained from this expression. Note from this column that there is a substantial reduction in first hinge loads for large enough cracks, $a/t \geqslant 0.3$, and for locating the crack at $\alpha = 0°$.

Finally, the influence of crack location on first hinge formation and its location (not necessarily at the crack) is of interest here. These results may be obtained using the superposition method of Fig. 3, but with the hinges and crack element at a position α from the three-o'clock position as indicated in Fig. 1. The results are in Table 4.

In Table 4, note that it has been assumed that the crack is into the inside or outside of the ring, so that it is on the tension side for each location, α. Also notice that the first hinge occurs at the crack location, when that location is at a relatively high moment in the uncracked ring, that is, $\theta = 0°$ to 15° and $\theta = 75°$ to 90°. However, for locations with relatively low moment, the first hinge forms at the maximum moment location, $\theta = 90°$. Finally, it is noted that the first hinge load, P_1, is affected appreciably only when the first hinge forms at the crack location. Of course, the largest reduction in relative load, P_1/P_I, is for placing the crack at the maximum moment point, $\theta = 90°$. Upon comparing the values of M/PR in Table 4 with Table 1, the effects of the changes of elastic stiffness of the "crack element" are also noted to be appreciable only when the crack is placed at a relatively high moment position. Of course, this effect would increase with larger a/t values ($a/t = 0.3$ in Table 4), but for this example it is really quite small.

3. Development of the second plastic hinge

In an uncracked ring, the second hinge develops at the same time as the first hinge, at the load points or points of maximum moment. Therefore, the second hinge load, P_{II}, for the uncracked ring is

$$P_{II} = P_I = \frac{\pi M_p}{R}. \tag{5}$$

The load for second hinge formation will be measured against this same relative load, P_I.

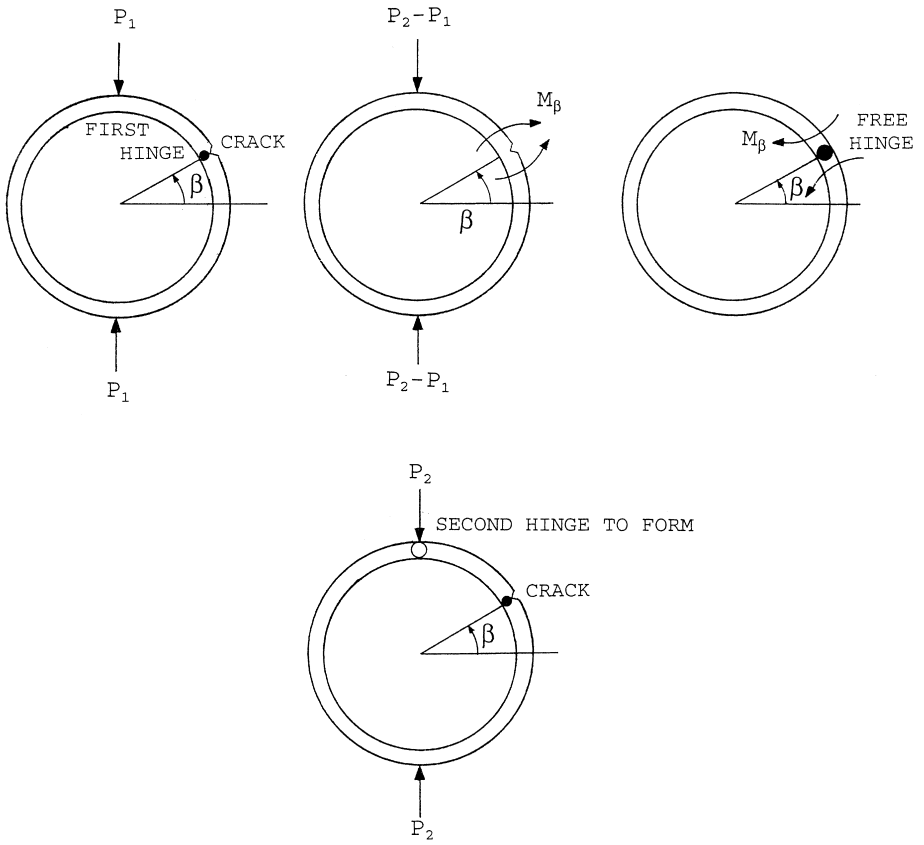

Fig. 4. Formation of the second hinge.

Again, the elastic superposition method can be used even though a first hinge is already formed. This is explained using Fig. 4.

From the situation just at the formation of the first hinge (first ring in Fig. 4), one may add the solution for an uncracked ring (second ring in Fig. 4) with a load increase, $P_2 - P_1$, but that adds a moment, M_β, at the first hinge location, β. Since no moment, M_β, should be added at a hinge, subsequently, the solution of a ring hinged at β with opposite moment, M_β, must be added (third ring in Fig. 4) to keep the proper hinge moment at the first hinge. The $P_2 - P_1$ added is determined by having it just attain the yield moment at some location other than β in the ring (last ring in Fig. 4). This gives exactly the ring result when the first hinge forms at the crack. For the cases where the first hinge does not form at the crack, the elastic stiffness change of the crack should be included to be exact. However, comparing Tables 1 and 4, the effect of those changes are very small for the cases where first hinges do not form at the crack ($\alpha = 30°$ to $60°$). Consequently, they shall be neglected in this example. Of course, it is possible to account for them using an additional superposition in the nature of Fig. 2.

With the preceding assumptions, Table 5 has been prepared. It is noted that the resulting second hinge locations are all at load points. For the symmetric case of $\alpha = 0°$, the hinges form at 90° and 270°, simultaneously. For the cases where the cracks are at relatively low moment locations, $\alpha = 30°$, 45°, and 60°, the hinge at 90° forms first and at 270° second, but within a 1% change in load, almost simultaneously, except for the slight influence of reduced elastic stiffness at the crack location. However, for cases of $\alpha = 0°$ and 15°, the hinges at the crack locations tend to reduce the moments at the load points

Table 5
θ and values of M/PR (for $a/t = 0.3$, and $R/t = 10$)

α	θ									P_2/P_1	P_2/P_1	Second hinge
	0°	15°	30°	45°	60°	75°	90°	180°	270°			
0°	0.150	0.132	0.089	0.010	−0.083	−0.189	−0.305	0.178	−0.305	1.04	1.18	90°, 270°
15°	0.169	0.153	0.103	0.027	0.079	0.188	−0.312	0.179	−0.295	1.01	1.04	90°
30°	0.181	0.164	0.114	0.035	−0.067	−0.189	−0.318	0.182	−0.318	1.00	1.00	270°
45°	0.181	0.164	0.114	0.035	−0.667	−0.189	−0.318	0.182	−0.318	1.00	1.00	270°
60°	0.181	0.164	0.114	0.035	−0.067	−0.189	−0.318	0.182	−0.318	1.00	1.00	270°
75°	0.183	0.174	0.131	0.038	−0.050	−0.172	−0.302	0.169	0.351	0.90	1.13	270°
90°	0.150	0.169	0.157	0.112	0.004	−0.100	−0.235	0.150	−0.480	0.66	1.37	270°

resulting in a slightly higher load required to form the second hinge (see P_2/P_1). On the other hand, when the crack is placed near or at the load point, $\alpha = 75°$ and 90°, the load to form the second hinge is substantially reduced (see P_2/P_1), but not nearly so much as the load to form the first hinge was reduced (see Table 4).

4. Development of the third plastic hinge

Once again, the formation of the full analysis at the instant of development of the third plastic hinge can be done using elastic superposition of results from "standard solutions". The approach used is shown in Fig. 5.

The analysis begins with the solution for the first two hinges as in Table 5. For the crack location, $\alpha = 0°$, the third hinge is already formed and nothing need be added. For other crack locations ($\alpha \neq 0°$), the solution for a full elastic ring with an increment of load, $P_3 - P_2$, is added. But this adds moments M_1 and M_2 at points where the first two hinges have formed. One can then add the solution to a ring with two free hinges with two opposite moments, M_1, and M_2 applied to cancel the increase in moments at the original plastic hinges. The load, P_3, is then adjusted so that the maximum moment at all positions away from the first two hinges in the summed solution just reaches the plastic hinge moment. Notice that the solution to the ring with two free hinges loaded by M_1 and M_2 can be formulated by the superposition of two solutions to the ring with a single hinge, so actually no new standard solutions are required here.

For the border perspective, it is more relevant to combine Tables 4–6 into a composite of the sequence of hinge formation as affected by the crack location. This is given as Table 7. The notations, 1 through 4, indicate the first through fourth hinges formed, respectively. The notations, 2, 3, and 3, 4 indicate simultaneous formation of two hinges, symmetric case of no crack.

Indeed, the widely varied pattern of the sequence of hinge formation in Table 7 is quite surprising. Simply, the change of the crack location (for a given crack size, $a/t = 0.3$, and ring slenderness ratio, $R/t = 10$) causes this wide variation in the pattern. Moreover, except for having the crack at the load point, $\alpha = 90°$, the relative loads for hinge formation do not vary greatly (less than 10% except for the first hinge for $\alpha = 75°$, near the load point). This seems quite surprising in view of the wide variety of hinge sequences.

One can further note here that the fourth (last) hinge forms either at 180° or 0°, which means that an elastic path connects the load points up until the fourth hinge forms. Since this method computes the elastic bending moments on that elastic path, the relative load point displacements can easily be computed for each successive hinge formation load, including the fourth hinge. Thus, a complete load–displacement diagram may be constructed, since that diagram will be linear between successive hinge formation loads.

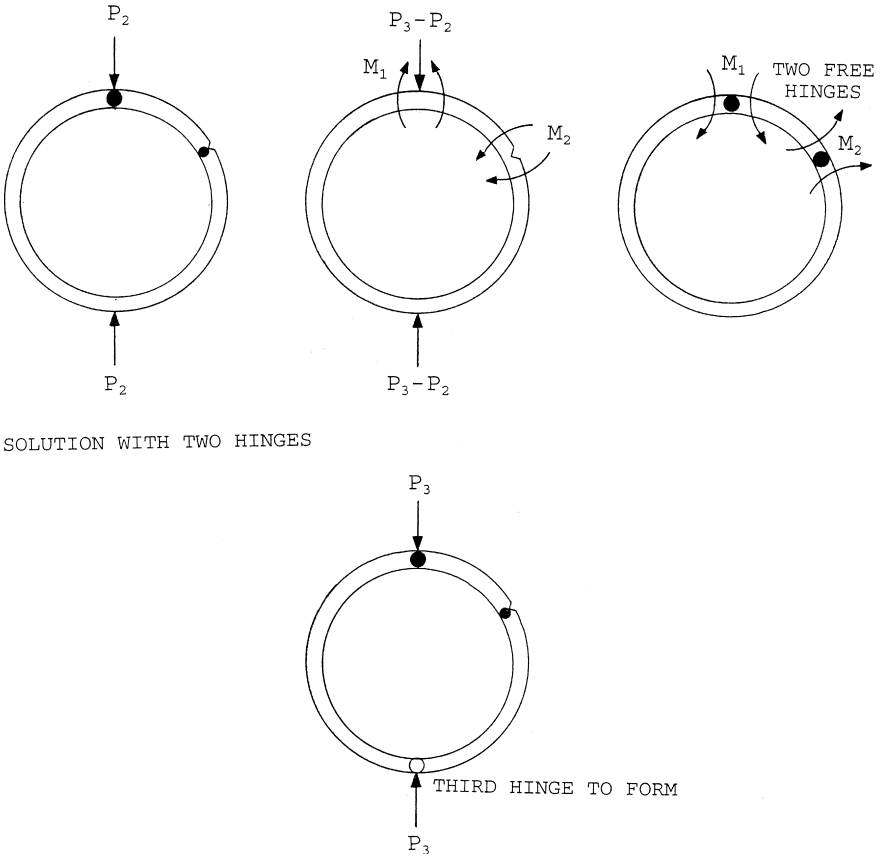

Fig. 5. Formation of the third hinge.

5. Crack stability with plastic hinges present

The stability of a crack in a ring with a plastic hinge at the crack is of interest here. For a crack when the crack location remains elastic, the stability analysis is regarded as well known and not considered here. In the ring problem, a method of tearing crack stability for at least a plastic hinge at the crack with the possibility of one or two (or none) additional plastic hinges at other locations in the ring will be developed. Development of a fourth hinge loads to plastic collapse (unstable), so it is not of relevance. The development will again make use of elastic superposition in the analysis. This type of superposition method was first given in Paris and Tada (1983) and Kaiser and Carlsson (1983) and is, as yet, not widely known. The stability analysis is explained here using Fig. 6. In this figure, the explanation starts with a ring with a plastic hinge at the crack size, a, and another plastic hinge, shown at the upper load point.

Now, if the crack size should increase by Δa, then the hinge moment at the crack will be reduced by $-\Delta M_{\mathrm{pCR}}$, while at the additional hinge no moment change occurs (provided additional deformation occurs in the same direction). Also, the load can be taken to stay constant (for dead-weight loading). Therefore, the "change state" to be added to the original state to get the final state is shown in the second ring of Fig. 6. In the "change state", additional plastic hinges are free hinges so that the hinge moment, M_{p}, does not change from the original state to the final state (however, if an additional hinge unloads during the change, it should be replaced by no hinge, or a locked hinge since elastic unloading will occur). At the plastic hinge

Table 6
θ and values of M/PR (for $a/t = 0.3$, and $R/t = 10$)

α	θ									P_3/P_1	P_3/P_2	Thid hinge
	0°	15°	30°	45°	60°	75°	90°	180°	270°			
0°	0.150	0.132	0.089	0.010	−0.083	−0.189	−0.305	0.178	−0.305	1.04	1.00	90°, 270°
15°	0.165	0.150	0.103	0.028	−0.070	−0.183	−0.305	0.202	−0.305	1.03	1.02	270°
30°	0.216	0.198	0.147	0.065	−0.040	−0.166	−0.300	0.216	−0.300	1.06	1.06	30° (C)
45°	0.280	0.261	0.203	0.116	−0.001	−0.135	−0.281	0.281	−0.281	1.13	1.13	180°, 0°
60°	0.280	0.261	0.203	0.116	−0.001	−0.135	−0.281	0.281	−0.281	1.13	1.13	180°, 0°
75°	0.264	0.247	0.195	0.097	−0.002	−0.132	−0.269	0.224	0.269	1.02	1.30	90°
90°	0.371	0.377	0.342	0.267	0.129	−0.012	−0.176	0.371	−0.371	0.88	1.33	0°, 180°

(C) indicates at crack.

Table 7
θ at hinge locations (for $a/t = 0.3$, and $R/t = 10$)

α	θ								P_1/P_1	P_2/P_1	P_3/P_1
	0°	15°	30°	45°	60°	75°	90°	180°	270°			
0°	*1*						2, 3	4	2, 3	0.88	1.04	1.04
15°		*1*					2	4	3	0.97	1.01	1.03
30°			*3*				1	4	2	1.00−	1.00+	1.06
45°	4						1	3	2	1.00−	1.00+	1.13
60°	4						1	3	2	1.00−	1.00+	1.02
75°						*1*	3	4	2	0.80	0.90	1.02
90°	3, 4						*1*	3, 4	2	0.48	0.66	0.88
No Crack	3, 4						1, 2	3, 4	1, 2	1.00	1.00	1.27

Italicized terms indicate diagonal crack location.

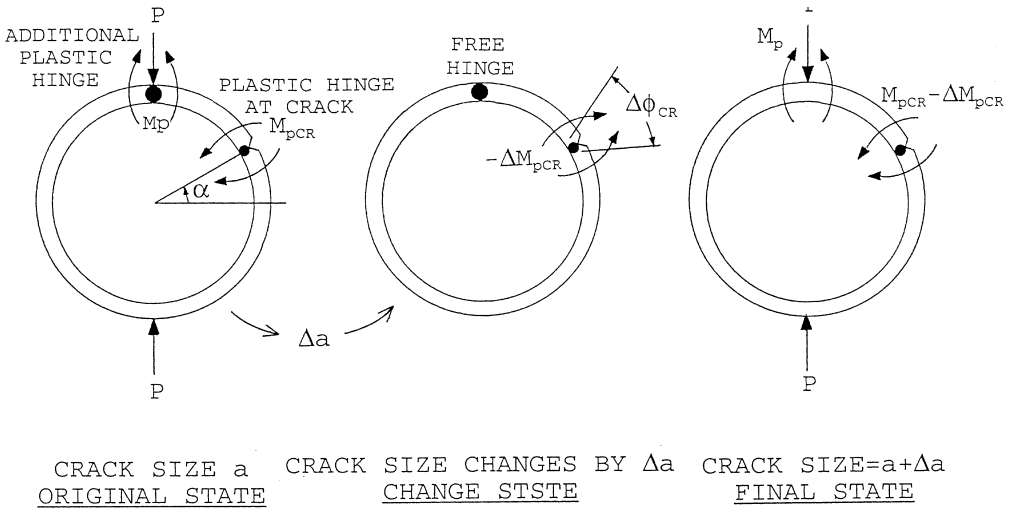

Fig. 6. Illustration of superposition.

at the crack with crack growth, Δa, the hinge moment is reduced, $-M_{\mathrm{pCR}}$, so an additional rotation of the hinge at the crack $\Delta\phi_{\mathrm{CR}}$ will occur. This additional deformation can cause the crack to advance further yet to drive the crack extension. Thus, the $\Delta\phi_{\mathrm{CR}}/\Delta M_{\mathrm{pCR}}$ in the "change state" controls whether the crack will be stable or not, and can be computed for the elastic ring with free hinges with ΔM applied at the crack site to get $\Delta\phi$ there. That is simple elastic structural calculation, so it shall be denoted as such

$$\frac{\Delta\phi}{\Delta M|_{\mathrm{structure}}} = \frac{\Delta\phi_{\mathrm{CR}}}{\Delta M_{\mathrm{pCR}}} = \text{negative} \tag{6}$$

and will result in a "negative" value as noted.

Now, the tendency toward instability as just noted is resisted by the material element containing the crack. That element with a crack could simply be tested for its resistance. Fig. 7 gives the nature of that test, where we simply take a cracked element with a crack of the correct initial size from a ring of the material (and ambient conditions) of interest. It is loaded with pure moment, M, at its ends and the rotation due to the presence of the crack, ϕ, is to be measured. The M versus ϕ so obtained will first reach a horizontal asymptote, if a plastic hinge is formed (as assumed as a precondition here). As crack growth begins to occur, the M versus ϕ curves will turn downward (either gradually or abruptly) and later always exhibits a lesser scope of decent, so that a maximum rate of decent, $\Delta M/\Delta\phi|_{\max}$ or minimum, $\Delta\phi/\Delta M|_{\text{material element}}$, for the material element may be identified. Now, the crack will remain stable if the structure sheds moment faster at the cracked section for a given $\Delta\phi$, than the material element does. That is

$$\left|\frac{\Delta\phi}{\Delta M}\right|_{\text{structure}} < \left|\frac{\Delta\phi}{\Delta M}\right|_{\text{material element}} \tag{7}$$

implies stable, where absolute values (not negative values) are compared. Since the minimum value of the material element's resistance is used, this criteria guarantees crack stability independent of the amount of hinge rotation at the cracked section.

However, as hinge rotation, ϕ, occurs with crack growth, the plastic hinge moment, M_{pCR}, will be reduced, which might cause changes in plastic hinge patterns such as the sequence of hinges. That can be assessed but will be left for later work.

On the other hand, it is of further interest here to evaluate $|\Delta\phi/\Delta M|_{\text{structure}}$ for the hinge patterns demonstrated in Table 7 for our example problem of a ring with diametrically opposite concentrated loads. That evaluation is to be done for the change state model in Fig. 6. Referring to Table 7, three cases occur when one of the first three hinges form at the crack location. These cases are shown in Fig. 8. They are discussed in terms of their specific relevance; see Table 7.

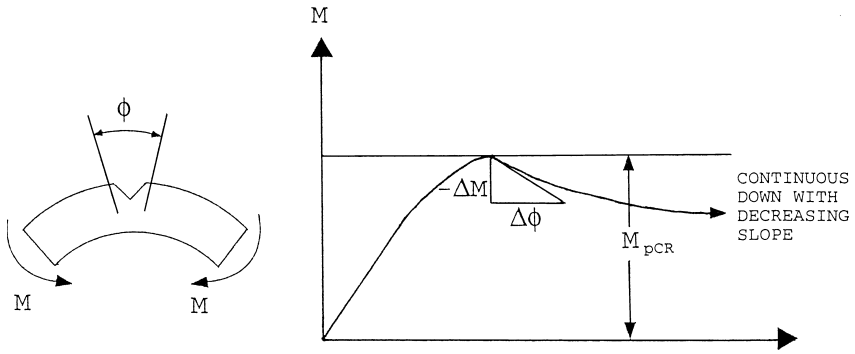

Fig. 7. Response of cracked element.

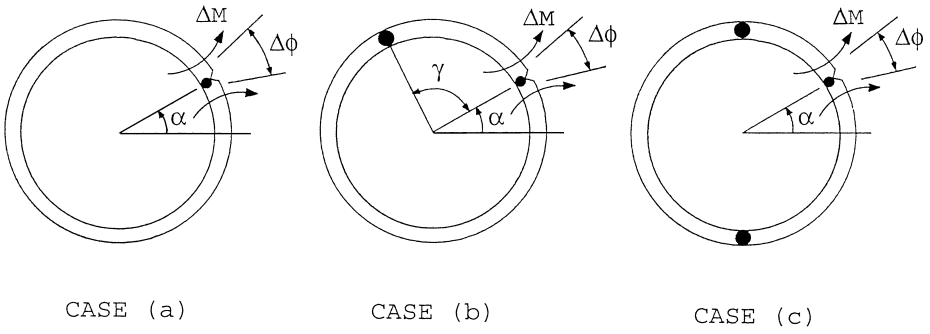

Fig. 8. Three cases for which one of the hinges forms at the crack (all rings with free hinges and ΔM applied).

Case (a): This applies to all situations where the first hinge forms at the crack location, that is, $\alpha = 0°,\ 15°, 75°,$ and $90°$. Analysis leads to

$$\frac{\Delta\phi}{\Delta M} = \frac{12R}{Et^3}\left[\frac{2}{3}\pi\right]. \tag{8}$$

Case (b): This applies to all situations where one of the first two hinges forms at the crack and a second forms (but not a third simultaneously) at an arbitrary location γ. This applies to $\alpha = 15°$, $75°$, and $90°$ in Table 7 where $\gamma = 75°,\ 165°,$ and $180°$, respectively. Analysis leads to

$$\frac{\Delta\phi}{\Delta M} = \frac{12R}{Et^3}\left[\frac{6\pi}{9 - (1 + 2\cos\gamma)^2}\right]. \tag{9}$$

Case (c): This applies to situations where three hinges are formed, one at the crack. Note that for all of these hinge cases (but not four simultaneously) that the non-crack location hinges are 180° apart in Table 7. Analysis leads to

$$\frac{\Delta\phi}{\Delta M} = \frac{12R}{Et^3}\left[\frac{\pi}{\cos^2\alpha}\right]. \tag{10}$$

Eqs. (8)–(10) cover all the cases in Table 7 where a hinge has formed at a crack. Eq. 8 is appropriate where one hinge is present and applies as $|\Delta\phi/\Delta M|_{\text{structure}}$ for the loads from first hinge formation up to second hinge formation. Similar load limits apply to Eqs. (9) and (10), so that as the loads are applied and hinges develop, each is relevant to load intervals between hinge formation. It is noted that these formation for $\Delta\phi/\Delta M$ do not contain the load explicitly or, for that matter, the crack size (which is contrary to fracture mechanics in the elastic range).

6. The use of elastic–plastic fracture mechanics *J*-integral methods for predicting material element behavior analysis

The experimental method for determination of $\Delta\phi/\Delta M|_{\min}$ for the material element containing the crack, as depicted in Fig. 7, is the "true" way to determine this quantity for a given initial crack size. However, a practical (conservative) approximation for this quantity may be obtained through a *J*-integral analysis making use of a *J*-integral analysis for material properties.

Let the *J*-integral for this application to bending be defined by its compliance from Rice (1967) or

$$J = -\int \left.\frac{\partial M}{\partial a}\right|_{\phi} \mathrm{d}\phi. \tag{11}$$

Under plastic hinge conditions at the crack site and assuming no hardening of the material, the moment, M, is the limit moment, M_{L}, which depends on crack size but not on ϕ. Therefore,

$$-\left.\frac{\partial M}{\partial a}\right|_{\phi} = -\frac{\mathrm{d}M_{\mathrm{L}}}{\mathrm{d}a} = \frac{\mathrm{d}M_{\mathrm{L}}}{\mathrm{d}b}, \tag{12}$$

where a is the crack size and b is the remaining uncracked ligament size at the cracked section. From Eqs. (11) and (12), it follows that

$$\mathrm{d}J = \frac{\mathrm{d}M_{\mathrm{L}}}{\mathrm{d}b}\mathrm{d}\phi. \tag{13}$$

Further, by definition,

$$\mathrm{d}M_{\mathrm{L}} = \left(\frac{\mathrm{d}M_{\mathrm{L}}}{\mathrm{d}a}\right)\mathrm{d}a = -\left(\frac{\mathrm{d}M_{\mathrm{L}}}{\mathrm{d}b}\right)\mathrm{d}a. \tag{14}$$

Combining Eqs. (12) and (14), it is found that

$$\left.\frac{\Delta\phi}{\Delta M}\right|_{\text{material element}} = \frac{\mathrm{d}\phi}{\mathrm{d}M_{\mathrm{L}}} = \frac{-\left(\frac{\mathrm{d}j}{\mathrm{d}a}\right)}{\left(\frac{\mathrm{d}M_{\mathrm{L}}}{\mathrm{d}b}\right)^2}. \tag{15}$$

As noted previously with Eq. (7), it is appropriate to take the absolute value, neglecting the negative sign in Eq. (15), and to use this result to obtain a minimum value for the material element to assume crack stability. That is to say we should insert a maximum value for $\mathrm{d}M_{\mathrm{L}}/\mathrm{d}b$ and a minimum value for $\mathrm{d}J/\mathrm{d}a$. Since M_{L} can only increase with b, it is conservative to use the value associated with the initial crack size (unless further sophistication is warranted).

The $\mathrm{d}J/\mathrm{d}a$ value to be used is to be found from the material's J-integral R-curve. On such an R-curve, $\mathrm{d}J/\mathrm{d}a$ is the slope of the curve, after initiation of crack growth, and usually the slope gradually diminishes with growth of the crack. Indeed, Eq. (11) may be used with the plastic hinge analysis methods here to find a $J_{\max}$ associated with $\phi_{\max}$ at the hinge. Then this $J_{\max}$ can be used to enter the R-curve to obtain $\mathrm{d}J/\mathrm{d}a$ for this hinge at the crack for any number of hinges short of final collapse.

However, adopting the J-modified method of Ernst (1983) for analysis of R-curve material property data, it is noted that a plot of that data on J versus $\mathrm{d}J/\mathrm{d}a$ (or T) diagram may be empirically bounded (minimum values) by a rectangular hyperbola, that is

$$(J)\left(\frac{\mathrm{d}J}{\mathrm{d}a}\right) = h \text{ (constant)}. \tag{16}$$

Taking an appropriate value of h from the available data, then

$$\frac{\mathrm{d}J}{\mathrm{d}a} = \frac{h}{J}. \tag{17}$$

Again, making use of Eq. (11) to find $J_{\max}$ for plastic hinge conditions at the crack site, the result is

$$J_{\max} = \frac{\mathrm{d}M_{\mathrm{L}}}{\mathrm{d}b}\phi_{\max} - J_0, \tag{18}$$

where J_0 is a constant accounting for passing through the elastic range while developing limit conditions that may be conservatively neglected. Then Eq. (18) leads to

$$J_{\max} \leqslant \frac{\mathrm{d}M_{\mathrm{L}}}{\mathrm{d}b}\phi_{\max}, \tag{19}$$

where upon Eq. (17) gives

$$\left(\frac{\mathrm{d}J}{\mathrm{d}a}\right)_{\min} \geqslant \frac{h}{\frac{\mathrm{d}M_{\mathrm{L}}}{\mathrm{d}b}\phi_{\max}}, \tag{20}$$

which may be used conservatively to evaluate $\Delta\phi/\Delta M$ in Eq. (15). Note that the $\phi_{\max}$ used in Eq. (20) is the maximum hinge rotation at the crack site for each appropriate partially developed hinge mechanism, as analyzed herein, short of collapse.

If this method using J-integral R-curve data shows the crack is stable, then it has done so conservatively, but with two reservations. First, it is assumed that the application itself is to a circumstance where the R-curve data is of higher (or equal) constraint conditions (toward plane strain). Second, it is also assumed that the application is made to conditions where J-controlled growth applies by Hutchinson and Paris (1979); that is

$$\frac{\mathrm{d}J}{\mathrm{d}a}\frac{b}{J} \gg 1 \tag{21}$$

for the application, otherwise further considerations must be invoked to use the J method. However, the method discussed in the previous section, associated with Fig. 7, of evaluating a cracked element of a ring directly has no such limitations.

Acknowledgements

This work, sponsored by the National Science Council, Republic of China, through the Grant NSC 88-2212-E-216-003 at Chung-Hua University is greatly acknowledged.

References

Ernst, H.A., 1983. Material resistance and instability beyond J-controlled crack growth. In: Shih, C.F., Gudas, J.P. (Eds.), Inelastic Crack Analysis, second symposium, vol. I, Elastic–Plastic Fracture, ASTM STP 803, American Society for Testing and Materials, Philadelphia, I-191–I-213.

Hutchinson, J.W., Paris, P.C., 1979. Stability analysis of J-contracted crack growth. In: Landes, J.D., Begley, J.A., Clarke, G.A. (Eds.), Elastic–Plastic Fracture, ASTM STP 668, American Society for Testing and Materials, Philadelphia, pp. 37–64.

Kaiser, S., Carlsson, A.J., 1983. Studies of different criteria for crack growth stability in ductile materials. In: Shih, C.F., Gudas, J.D. (Eds.), Fracture Curves and Engineering Applications, second symposium, vol. II, Elastic–Plastic Fracture, ASTM STP 803, American Society for Testing and Materials, Philadelphia, pp. II-58–II-79.

Paris, P.C., Tada, H., 1983. The application of fracture proof design methods using tearing instability theory to nuclear piping postulating circumstances through wall cracks. NUREG/CR-3464, US Nuclear Regulator Commission, Washington, DC.

Rice, J.R., 1967. Stresses due to a sharp notch in a work-hardening elastic–plastic material loaded by longitudinal shear. J. Appl. Mech. 34, 287–298.